DOI 10.1007/s11237-019-09602-9
Theoretical and Experimental Chemistry, Vol. 55, No. 2, May, 2019 (Russian Original Vol. 55, No. 2, March-April, 2019)

PLASMON EFFECT OF Ag NANOPARTICLES ON FÖRSTER RESONANCE ENERGY TRANSFER IN A SERIES OF CATIONIC POLYMETHINE DYES

E. V. Seliverstova,[1] **D. A. Temirbayeva,**[1]
N. Kh. Ibrayev,[1] **and A. A. Ishchenko**[2]

UDC 535.372; 535.341; 535.016

Enhanced Förster resonance energy transfer was found for donor–acceptor pairs of cationic dyes in the presences of silver nanoparticles (NPs) in solution. This enhancement is attributed both to an increase in the fluorescence intensity of the dyes and the direct effect of local plasmon resonance of the NPs on the energy transfer rate constant. Even in the case of low energy transfer efficiency, a significant increase in the rate constant of this process in the presence of silver NPs was found to be possible.

Key words: *Ag nanoparticles, energy transfer (FRET), polymethine dyes, plasmon effect.*

The intermolecular energy transfer of electronic excitation is one of the key processes in the transformation of absorbed light energy into other energy forms [1]. Depending on the type of interaction of the reacting species, energy transfer is accomplished either through an exchange mechanism or an inductive resonance mechanism [2]. It was theoretically predicted that localized surface plasmon resonance of metal nanoparticles (NPs) should strongly affect inductive resonance energy transfer (Förster resonance energy transfer, FRET) [3, 4]. Various workers [5-7] have shown that the rate of energy transfer can be either increased or decreased depending on the size, shape, and arrangement of the metal NPs relative to the donor–acceptor pair.

FRET is presently used in sensors [8, 9] as well as light-collecting [10, 11] and light-emitting structures [12]. Various workers [6, 13] have shown that such energy transfer between light-emitting molecules enhanced by Ag NP plasmons permits an increase in the luminescence of the acceptor molecules. Plasmon-enhanced energy transfer is used in hybrid metal-semiconductor nanostructures in new active materials for light-emitting diodes (LED) [12, 14]. FRET has been studied on the level of individual molecules and particles in theoretical and experimental investigations [15-17]. However, this process has not been studied extensively for a broad class of compounds.

In the present work, we studied the plasmon effect of silver NPs on FRET in a series of cationic polymethine dyes.

The xanthine dye rhodamine 6G (**R6G**) and polymethine dyes **1** and **1a** were used as the energy donor. Dyes **1** and **R6G** contain functional groups capable of coordinating with Ag NPs. These dyes absorb light in the near UV spectral range

---

[1] Institute of Molecular Nanophotonics, Buketov Karaganda State University, University St., 28, Karaganda 100028, Republic of Kazakhstan. E-mail: evgnseliverstova@gmail.com.
[2] Institute of Organic Chemistry, National Academy of Sciences of Ukraine, Murmans'ka St., 5, Kyiv 02660, Ukraine. E-mail: al.al.ishchenko@gmail.com.

Translated from Teoreticheskaya i Éksperimental'naya Khimiya, Vol. 55, No. 2, pp. 105-111, March-April, 2019. Original article submitted April 4, 2019; revision submitted April 11, 2019.

(Fig. 1a,b) but differ strongly in their fluorescence quantum yield [18]. The position and shape of the absorption and fluorescence bands of unsubstituted dye **1a** are virtually identical to those of dye **1**. Dye **2** (a vinylog of **1**) served as the acceptor [18].

Energy transfer was studied in ethanol solution at constant concentration of the donor molecules (10^{-5} mol/L). The concentration of the acceptor molecules was varied from 10^{-6} to 10^{-4} mol/L, while the concentration of the silver NPs in the dye solutions was varied from $6 \cdot 10^{9}$ to $3 \cdot 10^{12}$ particles/L (from 10^{-14} to $5 \cdot 10^{-12}$ mol/L).

The silver NPs in ethanol were obtained by ablation of a silver target using the second harmonic of an Nd : YAG solid-state laser according to our previous procedure [19]. The data obtained using a Tescan Mira 3MLU scanning electron microscopy indicated that these nanoparticles are spherical. The concentration of the silver NPs in the working solution was $C_{\mathrm{Ag}} = 3 \cdot 10^{13}$ particles/L ($5 \cdot 10^{-11}$ mol/L). The mean nanoparticle diameter was determined by the dynamic light scattering method using a Malvern Nanosizer 90S analyzer to be 48 nm with standard deviation 14.84 nm.

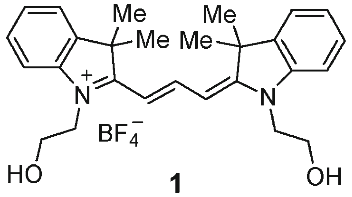

1

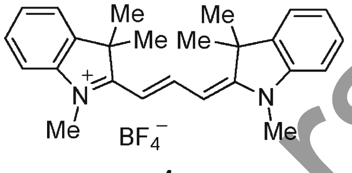

1a

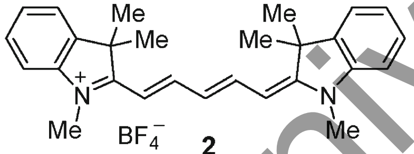

2

The absorption and fluorescence spectra of the samples were measured on Agilent Cary-300 and Eclipse spectrometers (manufactured in the USA), respectively. The fluorescence lifetimes of the donor and acceptor in the films were measured by the Becker & Hickl time-correlated photon-counting system (manufactured in Germany) at excitation wavelength $\lambda_{\mathrm{exc}} = 488$ nm. The fluorescence lifetimes were determined by treatment of the decay kinetics using the Becker & Hickl SPCImage program package (Germany). All the measurements were carried out in quartz cells with 2 mm pathlength at room temperature. The absolute fluorescence quantum yields (φ_{fl}) were measured using an Avantes integrating sphere (manufactured in the Netherlands) according to the procedure described by Wurth [20] and Suzuki [21].

The intensity decay of fluorescence was described by the formula

$$I(t) = \sum_{i=1}^{n} \alpha_i \exp(-t/\tau_i) \tag{1}$$

where τ_i is the decay lifetime, α_i is the amplitude or contribution fraction of the i-th component ($\sum_i \alpha_i = 1.0$).

The energy transfer efficiency (E_{ET}) was evaluated using the formula [2, 15]

$$E_{\mathrm{ET}} = 1 - \frac{\langle \tau_{\mathrm{D}} \rangle}{\langle \tau_{0\mathrm{D}} \rangle} \tag{2}$$

where $\langle \tau_{\mathrm{D}} \rangle$ and $\langle \tau_{0\mathrm{D}} \rangle$ are the mean fluorescence lifetimes of the donor without and with the acceptor determined as the sum of the products of the amplitudes and lifetimes of each component of the decay kinetics ($\Sigma\alpha_i\tau_i$).

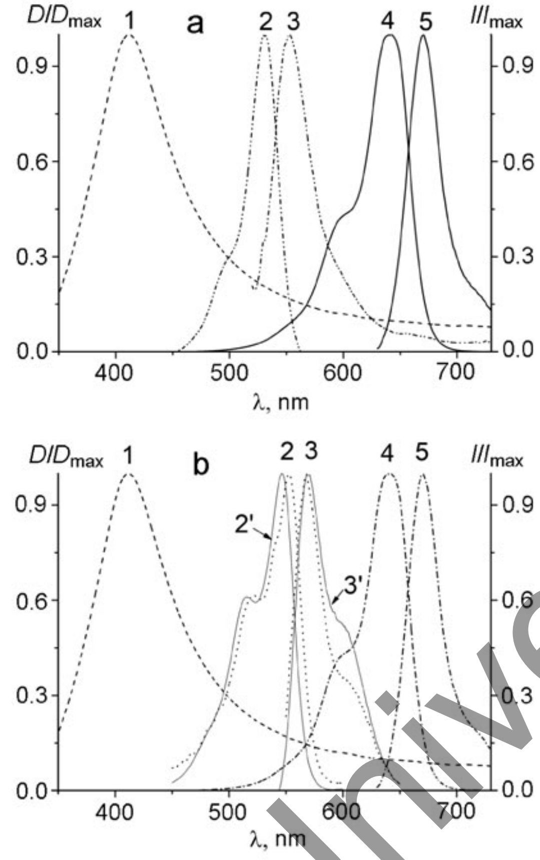

Fig. 1. Normalized absorption (1, 2, 2′, 4) and fluorescence spectra (3, 3′, 5) of ethanol solutions of silver NPs (1), energy donors **R6G** (2), **1** (3), **1a** (3′), as well as energy acceptors **2** (4, 5), pairs **R6G–1** (a), **1–2** (b), and **1a–2** (b).

The absorption band maximum of the silver NPs is at 412 nm and the band half-width is 88 nm (Fig. 1). The bands of the dyes and silver NPs overlap in Fig. 1a,b, which is a necessary condition for energy transfer. The absorption and emission spectra of dyes **1** are identical to the corresponding spectra of dye **1a**.

We studied the effect of silver NPs on the absorption and luminescence spectra of solutions of the individual dyes. These results are given in Table 1.

For all the dyes, there is no displacement of the absorption bands or change in their shape in the presence of Ag NPs. Also, there are no significant changes in the optical density (about 4%) for dyes **1**, **1a**, and **2**. An increase in optical density of 18% was found in the case of **R6G** when the nanoparticle concentration was $6 \cdot 10^{11}$ particles/L (10^{-12} mol/L). A further increase in the concentration of Ag NPs leads to a slight decrease in optical density.

The increase in optical density of the dyes may be related to an increase in the absorption cross-section by the action of the local field intensity near the surface of the metal nanoparticles. The absorption increases and reaches saturation with an increasing amount of Ag NPs in solution. Weakening of the field intensity may also occur with increasing concentration of plasmonics nanoparticles, which leads to a decrease in the absorption coefficient of the dye [22].

Table 1 shows that the addition of Ag NPs to the dye solutions leads to greater dye fluorescence intensity. The greatest intensity increase by almost 20% was found for $C_{\text{Ag}} = 3 \cdot 10^{11}$ particles/L ($5 \cdot 10^{-13}$ mol/L) both for **R6G** and dye **1** (Fig. 2a).

TABLE 1. Spectral-Luminescence Parameters of Solutions of Dyes **R6G**, **1**, **1a**, and **2** with Different Concentrations of Ag NP

C_{Ag}, particles/L (mol/L)	D	I, rel. units	$\langle \tau_{\text{fl}} \rangle$, ns	I/I_0
Rhodamine 6G				
0	0.11	11.36	4.2	–
$6\cdot10^{9}$ (10^{-14})	0.11	11.50	4.1	1.01
$3\cdot10^{10}$ ($5\cdot10^{-14}$)	0.11	11.56	4.1	1.02
$6\cdot10^{10}$ (10^{-13})	0.11	12.40	4.1	1.09
$3\cdot10^{11}$ ($5\cdot10^{-13}$)	0.12	13.40	4.1	1.18
$6\cdot10^{11}$ (10^{-12})	0.13	11.86	4.1	1.04
Dye **1**				
0	0.130	115	0.63	–
$1.8\cdot10^{10}$ ($3\cdot10^{-14}$)	0.131	120	0.63	1.04
$6\cdot10^{10}$ (10^{-13})	0.132	125	0.63	1.09
$3\cdot10^{11}$ ($5\cdot10^{-13}$)	0.132	136	0.62	1.18
$6\cdot10^{11}$ (10^{-12})	0.133	130	0.63	1.13
$1.8\cdot10^{12}$ ($3\cdot10^{-12}$)	0.135	116	0.62	1.01
Dye **1a**				
0	0.472	129	0.207	–
$1.8\cdot10^{10}$ ($3\cdot10^{-14}$)	0.483	132	0.202	1.02
$6\cdot10^{10}$ (10^{-13})	0.483	147	0.192	1.14
$3\cdot10^{11}$ ($5\cdot10^{-13}$)	0.483	133	0.198	1.03
$6\cdot10^{11}$ (10^{-12})	0.485	130	0.200	1.01
$1.8\cdot10^{12}$ ($3\cdot10^{-12}$)	0.483	125	0.202	0.97
Dye **2**				
0	3.98	1.24	0.97	–
$3\cdot10^{8}$ ($5\cdot10^{-15}$)	3.98	1.34	0.93	1.08
$6\cdot10^{9}$ (10^{-14})	3.98	1.39	0.93	1.12
$6\cdot10^{10}$ (10^{-13})	4.05	1.39	0.93	1.12
$3\cdot10^{11}$ ($5\cdot10^{-13}$)	4.12	1.37	0.93	1.10
$6\cdot10^{11}$ (10^{-12})	4.10	1.36	0.93	1.09

Note. D) optical density of dye at the absorption band maximum: 530 nm for **R6G**, 550 nm for **1** and **1a**, and 640 nm for **2**; I) fluorescence intensity at the emission band maximum: 555 nm for **R6G**, 565 nm for **1** and **1a**, and 670 nm for **2**; $\langle \tau_{\text{fl}} \rangle$ is the mean fluorescence lifetime, I/I_0 is the fluorescence enhancement factor defined as the ratio of the fluorescence intensity without and with Ag NPs.

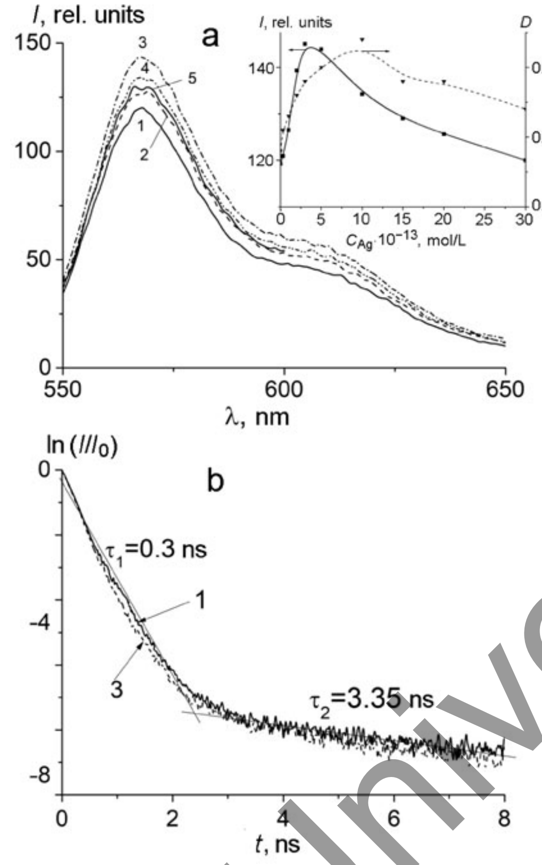

Fig. 2. Fluorescence spectra (a) and decay kinetics (b) of dye **1** in the presence of different concentrations of Ag NPs: 1) 0, 2) $6\cdot10^{10}$, 3) $3\cdot10^{11}$, 4) $9\cdot10^{11}$, and 5) $1.8\cdot10^{12}$ particles/L. The insert gives the dependence of the emission intensity and optical density of dye **1** on the concentration of Ag NPs.

Fluorescence enhancement of 14% was found for dye **1a** at $C_{\text{Ag}} = 6\cdot10^{10}$ particles/L (10^{-13} mol/L) and of 12% for **2** at the same concentration.

The more pronounced effect of Ag NPs on the fluorescence capacity of dyes **R6G** and **1** than for dyes **1a** and **2** is apparently due to the stronger interaction of the former with the nanoparticles since their functional groups can form coordination bonds with the NPs.

Various workers [3, 16, 23] have shown that the spectral effects depend strongly both on the distance and orientation between the dye molecule and metal NP. The slight increase in the optical density and fluorescence intensity of the dye in our case is related to the circumstance that the molecules are arranged randomly about the silver NPs and at random distance in the system studied. In this case, the amount of dye molecules reaching the field of localized surface plasmon resonance is insufficient to permit detection of a several-fold enhancement of the optical parameters.

The fluorescence decay kinetics of **R6G** and dye **2** is given by a monoexponential equation, while the corresponding decay kinetics for dye **1** is given by a biexponential equation (Fig. 2b). The contribution of the fast component (τ_1 = 0.3 ns) accounts for 99% of the total fluorescence decay time, while the slow component (τ_2 = 3.35 ns) accounts for only 1%. The fluorescence lifetime of all the dyes is almost unaffected by the addition of silver NPs.

The observed enhancement of fluorescence intensity of the dyes is probably related to a greater rate of radiative transition of the dye molecules from the S_1 to the S_0 state. Hence, we would expect that an increase in the fluorescence rate

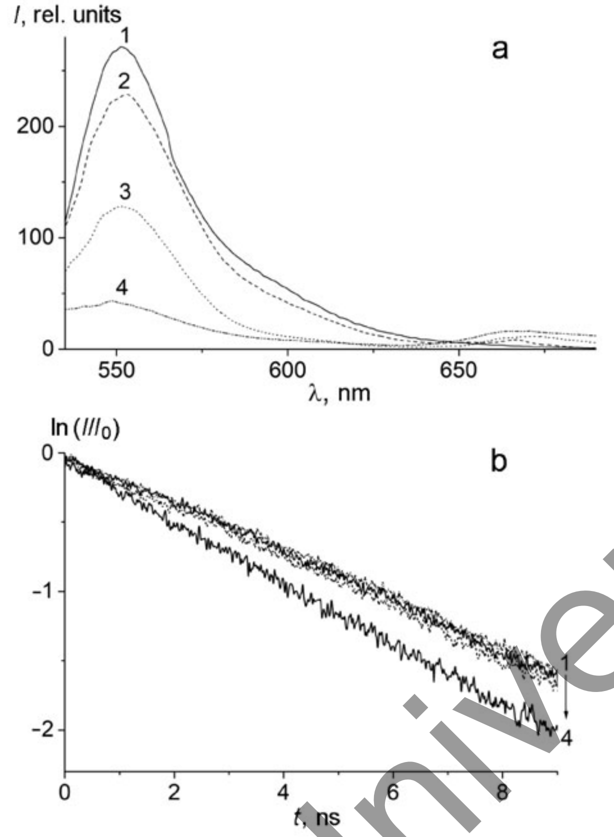

Fig. 3. Fluorescence spectra (a) and fluorescence decay kinetics (b) of **R6G** (1) and a mixture of **R6G** and **2** with different concentrations of **2**: 2) 10^{-6}, 3) 10^{-5}, and 4) 10^{-4} mol/L.

constant would lead to a decrease in the lifetime of the S_1 excited state. However, measurements showed that τ_{fl} of the dyes does not change with variation in the concentration of Ag NPs. This behavior is possible if there is a decrease in nonradiative deactivation of the S_1 state in the presence of metal NPs along with an increase in the efficiency of the radiative decay channel [23].

The fluorescence quenching at concentrations above $C_{Ag} = 6 \cdot 10^{11}$ particles/L (10^{-12} mol/L) appear to be related to energy transfer from the excited dye molecules to the metal NPs [24].

Since the effect of Ag NPs, as noted above, falls off in the series **R6G** > **1** > **1a** > **2** and the fluorescence lifetime of dye **1a** is almost three times less than for dye **1**, we limited ourselves to the dye pairs **R6G–2** and **1**–**2** in studying the effect of localized plasmon resonance on energy transfer. For this purpose, mixed donor–acceptor solutions were excited at the absorption band of the energy donor (λ_{exc} = 488 nm).

Fluorescence quenching and shortening of the fluorescence lifetime are observed upon the addition of the acceptor to a solution of **R6G** (Fig. 3). Fluorescence of the polymethine dye **2** appears in the red region of the spectrum. There is no fluorescence upon excitation of solutions of acceptor **2** at λ_{exc} = 488 nm. Thus, this long-wave emission should be assigned to sensitized fluorescence of the acceptor molecules, which appears as the result of energy transfer from singlet-excited donor molecules to acceptor molecules. The lack of distortion of the shape of the fluorescence spectrum of the donor due to the reabsorption of its emission as well as the significant decrease in the fluorescence lifetime of **R6G** and invariance of its τ_{fl} upon change in the recording wavelength indicate the lack of a significant contribution of a radiative channel for energy transfer.

TABLE 2. Fluorescence Lifetime τ_{fl} of **R6G**, Dye **1** and Dye **2** upon Excitation in the Donor Absorption Band (λ_{exc} = 488 nm)

Acceptor concentration, mole %	E_{ET}	τ_{fl}, ns			
		τ_{1D}	τ_{2D}	$\langle \tau_D \rangle$	τ_A
		R6G–dye **2**			
0	–	–	–	4.20	–
10^{-6}	0.02	–	–	4.10	3.2
10^{-5}	0.03	–	–	4.08	3.2
10^{-4}	0.20	–	–	3.40	3.2
		Dyes **1**–**2**			
0	–	0.3	3.3	0.33	–
10^{-6}	0.003	0.3	3.2	0.33	0.93
10^{-5}	0.03	0.3	2.45	0.32	0.93
10^{-4}	0.06	0.294	1.93	0.31	0.93

Note. E_{ET} is the energy transfer efficiency, τ_{1D} and τ_{2D} are the fast and slow components of the fluorescence decay kinetics of donor **1**, $\langle \tau_D \rangle$ is the mean fluorescence lifetime of **R6G** (λ_{reg} = 580 nm), of **1** (λ_{reg} = 605 nm), τ_A is the sensitized fluorescence lifetime of the acceptor at λ_{reg} = 655 nm; τ_{iD} values are not shown for **R6G** because its fluorescence kinetics is described by a monoexponential decay equation.

The fluorescence decay kinetics of donor **R6G** in the absence and presence of molecules of acceptor **2** also confirms energy transfer of electronic excitation between the dyes (Fig. 3b). The measured lifetimes for the fluorescence (τ_{fl}) of the donor and sensitized fluorescence of the acceptor as well as the energy transfer efficiency (E_{ET}) are given in Table 2. Fluorescence quenching of donor dye **1** and the appearance of sensitized emission of dye **2** were detected between polymethine dyes **1** and **2**, as in the case of **R6G** and **2** (Table 2). The decay kinetic curve for dye **1** is described by a biexponential equation and consists of two components, namely, a fast component with τ_{1D} and slow component with τ_{2D}. When energy transfer takes place, the predominant quenching is observed through the second slower component. In this case, the contribution of τ_{1D} in all cases was 0.99 and the contribution of τ_{2D} was only 0.01.

The spectral kinetic measurements were carried out on the donor–acceptor solutions with and without silver NPs (Table 3). The acceptor molecule concentration in this case was 10^{-4} mol/L. The energy transfer rate constant k_{ET} was found using the method Zhang et al. [15] using the data for the energy transfer efficiency E_{ET} and donor fluorescence lifetime τ_{0D}.

Table 3 shows that the energy transfer efficiency in the case of the pair of dyes **1** and **2** is much lower than for the pair of **R6G** and **2**. This finding may be related both to a lower value of the fluorescence and absorption band overlap integral for the **1–2** pair (Table 4) and the lower quantum yield φ_{fl} of energy donor dye **1** than for **R6G**. The value for φ_{fl} is 0.92 for **R6G** but only 0.08 for dye **1**.

In addition, enhanced energy transfer efficiency is observed for both donor–acceptor pairs in the presence of silver NPs. The maximum increase in the energy transfer efficiency E_{ET} in this case is noted in comparison with energy transfer without Ag NPs. The value of E_{ET} was enhanced by 45% and 50% for the pairs **R6G–2** and **1–2**, respectively. This finding could presumably be related to greater overlap integrals of the absorption bands of the donor–acceptor dye pairs and the

TABLE 3. Fluorescence Lifetime τ_{fl} of Energy Donors **R6G** and **1** upon Excitation in the Absorption Band of the Donor ($\lambda_{exc} = 488$ nm) and in the Presence of Acceptor **2** ($C = 10^{-4}$ mol/L) and Various Concentrations of Ag NPs

C_{Ag}, particles/L (mol/L)	τ_D, ns					E_{ET}	$k_{ET} \cdot 10^7$, s^{-1}
	τ_{1D}	α_1	τ_{2D}	α_2	$\langle \tau_D \rangle$		
			R6G–dye **2**				
0	–	–	–	–	3.40	0.2	4.76
$6 \cdot 10^9$ (10^{-14})	–	–	–	–	3.2	0.26	6.85
$3 \cdot 10^{10}$ ($5 \cdot 10^{-14}$)	–	–	–	–	3.0	0.29	7.97
$6 \cdot 10^{10}$ (10^{-13})	–	–	–	–	3.2	0.26	6.85
$3 \cdot 10^{11}$ ($5 \cdot 10^{-13}$)	–	–	–	–	3.25	0.23	5.83
$6 \cdot 10^{11}$ (10^{-12})	–	–	–	–	3.3	0.22	5.50
			Dyes **1–2**				
0	0.294	0.985	1.93	0.015	0.31	0.06	1.4
$9 \cdot 10^{10}$ ($1.5 \cdot 10^{-13}$)	0.287	0.987	2.2	0.013	0.31	0.06	0.97
$1.8 \cdot 10^{11}$ ($3 \cdot 10^{-13}$)	0.282	0.985	2.2	0.015	0.31	0.06	0.97
$3 \cdot 10^{11}$ ($5 \cdot 10^{-13}$)	0.278	0.986	2.04	0.014	0.30	0.09	1.42
$6 \cdot 10^{11}$ (10^{-12})	0.284	0.989	2.0	0.011	0.30	0.08	2.01
$2 \cdot 10^{-12}$	0.29	0.985	2.0	0.015	0.32	0.04	1.48

Note. E_{ET} is the energy transfer efficiency, τ_{1D} and τ_{2D} are the fast and slow components of the fluorescence decay kinetics of dye **1**, α_1 and α_2 are the amplitudes of the slow and fast components of dye **1**, τ_{iD} and α_i are not indicated for **R6G** since its fluorescence kinetics is described by a monoexponential equation, k_{ET} is the energy transfer rate constant.

fluorescence band of the Ag NPs (Table 4). However the integral was enhanced by only 14%-15% for both dye pairs. Thus, this effect cannot be the major reason for the enhanced E_{ET}.

We note that Ag NPs may form aggregates. However, even in the initial silver nanoparticle solution and after its dilution, we find absorption spectra with a distinct band and maximum at about 412 nm. In addition, a change in the half-width and shape of the spectrum should be observed upon aggregate formation but this was not found in our case. This result suggests that aggregate formation is unlikely. Furthermore, Schlucker [22] reported that the local field enhancement coefficient at the hot spot between particles at distances from 1 to 20 nm varies from $7 \cdot 10^3$ to $5 \cdot 10^5$. We might have expected a considerable increase in the dye luminescence. However, in the case of the dyes studied, only small enhancement coefficients are found. This result indicates that the enhancement of luminescence most likely occurs near the field of individual Ag NPs.

Thus, the efficiency of FRET between these organic dyes may be enhanced in the presence of silver NPs both due to increased fluorescence intensity of the dyes by the action of plasmonic nanoparticles and to a direct effect of the local plasmon resonance of the Ag NPs on the energy transfer rate constant. Evaluation of k_{ET} showed that despite initially low energy transfer efficiency, an increase in the energy transfer rate constant in the case of dyes **1** and **2** by almost 44% is observed in the presence

TABLE 4. Overlap Integral Values ($M^{-1}\cdot cm^3$) of the Absorption Spectrum of the Donor and the Fluorescence Spectrum of Acceptor in the Presence of the Ag NPs

C_{Ag}, mol/L	**R6G**–dye **2**	Dyes **1–2**
0	$9.1\cdot10^{-13}$	$6.3\cdot10^{-13}$
$1.8\cdot10^{10}$ ($3\cdot10^{-14}$)	$9.1\cdot10^{-13}$	$6.33\cdot10^{-13}$
$6\cdot10^{10}$ (10^{-13})	$9.7\cdot10^{-13}$	$6.98\cdot10^{-13}$
$3\cdot10^{11}$ ($5\cdot10^{-13}$)	$10.49\cdot10^{-13}$	$7.21\cdot10^{-13}$
$6\cdot10^{11}$ (10^{-12})	$10.20\cdot10^{-13}$	$7.06\cdot10^{-13}$

of silver NPs. The greatest increase in the energy transfer rate was about 67% when using **R6G** as the energy donor instead of dye **1**.

Hence, the fluorescence intensity of the dyes studied in the presence of Ag NPs increased by almost 20% for both energy donors and by 12% for the energy acceptor in comparison with the values in the absence of Ag NPs. On the other hand, the enhanced energy transfer efficiency in the presence of Ag NPs is 44% and 67% for both dye pairs studied. This finding indicates that E_{ET} is increased predominantly due to enhancement of the energy transfer rate constant.

This work was carried out with the financial support of the Ministry of Education and Science of the Republic of Kazakhstan (Grant No. BR05236691 for research on Nanoplasmonics: Synthesis of Nanostructures, Study of Their Properties and Current Applications).

REFERENCES

1. R. K. Clayton, *Photosynthesis: Physical Mechanisms and Chemical Patterns*, Cambridge Univ. Press, Cambridge (1980).
2. J. R. Lakowicz, *Principle of Fluorescence Spectroscopy*, Kluwer/Plenum Publ., New York (2006).
3. X. M. Hua, J. I. Gersten, and A. Nitzan, *J. Chem. Phys.*, **83**, 3650-3659 (1985), doi: 10.1063/1.449120.
4. F. Reil, U. Hohenester, J. R. Krenn, et al., *Nano Lett.*, **8**, 4128-4133 (2008), doi: 10.1021/nl801480m.
5. L. Zhao, T. Ming, L. Shao, et al., *J. Phys. Chem.*, **116**, 8287-8296 (2012), doi: 10.1021/jp300916a.
6. D. Bouchet, D. Cao, R. Carminati, et al., *Phys. Rev. Lett.*, **116**, 03740(1-5) (2016), doi: 10.1103/PhysRevLett.116.037401.
7. M. G. Kucherenko, V. N. Stepanov, and N. Yu. Kruchinin, *Opt. Spectrosc.*, **118**, 103-110 (2015), doi: 10.1134/S0030400X15010154.
8. S. K. Sekatskii, G. T. Shubeita, M. Chergui, et al., *J. Exp. Theor. Phys.*, **90**, 769-777 (2000), doi: 10.1134/1.559161.
9. A. V. Zayats and D. Richards (eds.), *Nano-Optics and Near-Field Optical Microscopy*, Artech House, Boston-London (2009).
10. N. Ibrayev, E. Seliverstova, A. Aimukhanov, et al., *Mol. Cryst. Liq. Cryst.*, **589**, 202-204 (2014); doi: 10.1080/15421406.2013.872827.
11. N. Ibrayev, E. Seliverstova, N. Nuraje, et al., *Mat. Sci. Semicon. Proc.*, **31**, 358-362 (2015), doi: 10.1016/j.mssp.2014.12.006.

12. D. H. Park, M. S. Kim, and J. Joo, *Chem. Soc. Rev.*, **39**, 2439-2452 (2010), doi: 10.1039/B907993A.
13. R. Mattew, M. C. Claire, Z. Jie, et al., *Chem. Rev.*, **111**, 3669-3712 (2011), doi: 10.1021/cr100275d.
14. Y. Lee, S. H. Lee, S. Park, et al., *Synth. Met.*, **187**, 130-135 (2014), doi: 10.1016/j.synthmet.2013.11.005.
15. J. Zhang, Fu Yi, and J. R. Lakowicz, *J. Phys. Chem. C*, **111**, 50-56 (2007), doi: 10.1021/jp062665e.
16. J. Zhang, Fu Yi, M. H. Chowdhury, et al., *J. Phys. Chem. C*, **111**, 11784-11792 (2007); doi: 10.1021/jp067887r.
17. M. L. Viger, D. Brouard, and D. Boudreau, *J. Phys. Chem. C.*, **115**, 2974-2981 (2011), doi: 10.1021/jp109993a.
18. A. A. Ishchenko, *Teor. Éksp. Khim.*, **34**, No. 4, 214-231 (1998). [*Theor. Exp. Chem.*, **34**, No. 4, 191-210 (1998) (English translation)], doi: 10.1007/BF02523249.
19. A. K. Aimukhanov, N. Kh. Ibraev, A. A. Ishchenko, and A. V. Kulinich, *Teor. Éksp. Khim.*, **54**, No. 6, 338-343 (2018). [*Theor. Exp. Chem.*, **54**, No. 6, 369374 (2019) (English translation)], doi: 10.1007/s11237-019-09583-9.
20. C. Wurth, M. G. Gonzalez, R. Niessner, et al., *Talanta*, **90**, 30-37 (2012); doi: 10.1016/j.talanta.2011.12.051.
21. K. Suzuki, A. Kobayashi, Sh. Kaneko, et al., *Phys. Chem. Chem. Phys.*, **11**, 9850-9860 (2009); doi: 10.1039/b912178a.
22. S. Schlucker (ed.), *Surface Enhanced Raman Spectroscopy: Analytical, Biophysical and Life Science Applications*, Wiley, Hoboken, NJ (2011).
23. P. Anger, P. Bharadwaj, and L. Novotny, *Phys. Rev. Lett.*, **96**, 113002(1-4) (2006); doi: 10.1103/PhysRevLett.96.113002.
24. C. D. Geddes and J. R. Lakowicz, *J. Fluorescence*, **12**, 121-129 (2002); doi: 10.1023/A:1016875709579.